Detection of Low Observable Targets Within Sea Clutter by Structure Function Based Multifractal Analysis

Jing Hu, Wen-Wen Tung, and Jianbo Gao, *Member, IEEE*

***Abstract*—Sea clutter is the backscattered returns from a patch of the sea surface illuminated by a radar pulse. Robust detection of targets within sea clutter may strengthen coastal security, improve navigation safety, and help environmental monitoring. However, no simple and reliable methods for detecting targets within sea clutter have been proposed. We introduce the structure function based multifractal theory to analyze 392 sea clutter datasets measured under various sea and weather conditions. It is found that sea clutter data exhibit multifractal behaviors in the time scale range of about 0.01 s to a few seconds, especially for data with targets. The fractal and multifractal features of sea clutter enable us to develop a simple and effective method to detect targets within sea clutter. It is shown that the method achieves very high detection accuracy. It is further shown that in the time scale range of 0.01 s to a few seconds, sea clutter data is weakly nonstationary. The nonstationarity may explain why modeling using distributions such as Weibull, log-normal, K, and compound-Gaussian only offers limited understanding of the physics of sea clutter and is not very effective in detecting targets within sea clutter.**

***Index Terms*—Fractal, radar, sea clutter, structure function based multifractal analysis, target detection.**

I. Introduction

SEA CLUTTER refers to the radar returns from a patch of ocean surface. Accurate modeling of sea clutter and robust detection of low observable targets within sea clutter are important problems in remote sensing and radar signal processing applications, for a number of reasons: 1) identifying objects within sea clutter such as submarine periscopes, low-flying aircrafts, and missiles can greatly improve our coastal and national security; 2) identifying small marine vessels, navigation buoys, small pieces of ice, patches of spilled oil, etc., can significantly reduce the threat to the safety of ship navigation; and 3) monitoring and policing of illegal fishing is an important activity in environmental monitoring.

Due to the fractal nature of sea surface profile, which is a consequence of energy transfer from small scale to large scale of sea surface wave, sea clutter is often highly non-Gaussian [1]–[10], even spiky [11], especially in heavy sea conditions. Hence, sea clutter modeling is a very difficult problem, and a lot of effort has been made to study sea clutter. Traditionally, sea clutter is often studied in terms of certain simple statistical features, such as the marginal probability density function (PDF). The non-Gaussian feature of sea clutter has motivated researchers to employ Weibull [1], log-normal [2]–[4], K [5]–[8], [12], and compound-Gaussian [9], [10] distributions to model sea clutter. However, such simple phenomenological modeling of sea clutter only offers limited analytical or physical understanding. In fact, we shall show later, distributional analysis is not effective in detecting targets within sea clutter.

Recently, to gain deeper understanding of the nature of sea clutter, the concept of fractal has been employed for the description and modeling of the roughness of sea surface [13]–[15], and investigation of scattering from rough surfaces modeled by fractal processes [16]–[19]. Possible chaotic behavior of sea clutter has also been studied [20]–[29].

Since the ultimate goal of sea clutter study is to improve detection of targets embedded within clutters, a lot of effort has been made to design innovative methods for target detection within sea clutter. Notable methods include time-frequency analysis techniques [30], wavelet based approaches [31], neural network based approaches [32]–[35], and wavelet-neural net combined approaches [36], [37], as well as utilizing the concept of fractal dimension [38] and fractal error [39], [40], and boxing-counting based multifractal analysis [41]. It appears that the most thoroughly evaluated scheme is the one based on a neural network model [34]. Note that most of the above works were based on the analysis of radar images. To improve detection accuracy, some researchers resort to higher resolution more powerful millimeter wave radars [42]. The status of the field clearly indicates that one needs to adopt a systematic approach, work on a large number of datasets measured under various wave height and weather conditions, and design a few readily computable parameters that can accurately and easily detect targets within sea clutter.

In this paper, we adopt advanced signal processing concepts and tools from random fractal theory to study sea clutter. Specifically, we apply the structure function based multifractal analysis to analyze 392 sea clutter data measured under various sea and weather conditions. It is found that sea clutter data exhibit multifractal behaviors in the time scale range of about 0.01 s to a few seconds, especially for data with targets. The fractal and multifractal features of sea clutter enable us to develop a simple and effective method to detect targets within sea clutter. It is shown that the method achieves very high detection accuracy. It

Manuscript received December 17, 2004; revised June 6, 2005. Presented in part at the IEEE International Conference on Acoustics, Speech, and Signal Processing (ICASSP), Philadelphia, PA, March 18–23, 2005.

J. Hu and J. Gao are with the Department of Electrical and Computer Engineering, NEB 413, University of Florida, Gainesville, FL 32611 USA (e-mail: jhu@ecel.ufl.edu, gao@ece.ufl.edu).

W.-W. Tung is with the Department of Earth and Atmospheric Sciences, Purdue University, West Lafayette, IN 47907 USA (e-mail: wwtung@purdue.edu).

Digital Object Identifier 10.1109/TAP.2005.861541

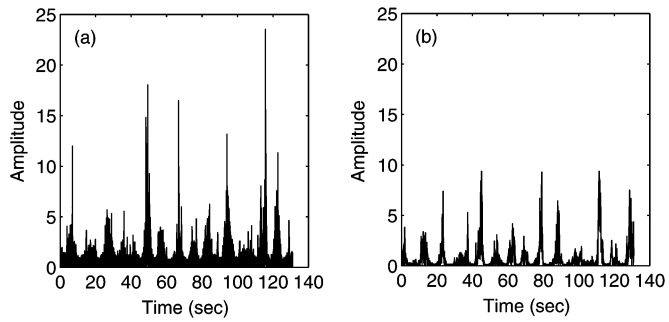

Fig. 1. Examples of the sea clutter amplitude data (a) without and (b) with target. (a) and (b) are plotted using range bin 1 and 9, HH polarization of data file 17 downloaded from the link given in Section II. The radial distance for the data plotted in (a) and (b) is 2574 m and 2694 m, respectively. The azimuth angle for both (a) and (b) is about 129°. Similar figures were shown in [27], [28].

is further shown that in the time scale range of 0.01 s to a few seconds, sea clutter data is weakly nonstationary.

The remainder of the paper is organized as follows. In Section II, we briefly describe the sea clutter data. In Section III, we introduce the structure function based multifractal analysis. In Section IV, we analyze the sea clutter data by using the structure function based multifractal analysis. The nonstationarity of sea clutter data stimulates us to carefully examine the data by fitting them according to the commonly used distributions for modeling sea clutter, such as Weibull, log-normal, K and compound-Gaussian distributions. In Section V, we show that indeed these distributions only offer limited understanding of the physics of sea clutter and are not very effective in detecting targets within sea clutter. Finally, some concluding remarks are made in Section VI.

II. Sea Clutter Data

We have obtained 14 sea clutter datasets from a website maintained by Professor Simon Haykin (http://soma.ece.mcmaster.ca/ipix/dartmouth/datasets.html). The measurement was made using the McMaster IPIX radar at the east coast of Canada, from a clifftop near Dartmouth, Nova Scotia. The operating (carrier) frequency of the radar is 9.39 GHz (and hence a wavelength of about 3 cm), with two polarizations, HH (horizontal transmission, horizontal reception) and VV (vertical transmission, vertical reception). The grazing angle varied from less than 1° to a few degrees. The wave height in the ocean varied from 0.8 m to 3.8 m (with peak height up to 5.5 m). The wind conditions varied from still to 60 km/hr (with gusts up to 90 km/hr). Each dataset contains 14 spatial range bins of HH as well as 14 range bins of VV datasets. Therefore, there are a total of 392 sea clutter time series. A few of the range bins hit a target, which was made of a spherical block of styrofoam of diameter 1 m, wrapped with wire mesh. Each range bin data contains 2^{17} complex numbers, with a sampling frequency of 1000 Hz. We analyze the amplitude data. Fig. 1 shows two examples of the sea clutter amplitude data without and with target.

III. Structure Function Based Multifractal Analysis

The structure function based multifractal analysis examines power-law relations for all orders of moments. It works as follows. Let $X = \{X_i, i = 1, 2, \ldots, N\}$ denote a covariance stationary stochastic process with mean μ and variance σ^2. We first subtract the mean from the time series. Denote the new time series as $x = \{x_i, i = 1, 2, \ldots, N\}$, where

$$x_i = X_i - \mu. \tag{1}$$

Then we form the partial summation of x to construct a new time series $y = \{y(n), n = 1, 2, \ldots, N\}$, where

$$y(n) = \sum_{i=1}^{n} x_i. \tag{2}$$

Often, y is called a "random walk" process of x, while x an "increment" process. One then examines whether the following scaling laws hold:

$$F^{(q)}(m) = \left\langle \left| y(n+m) - y(n) \right|^q \right\rangle^{1/q} \sim m^{H(q)} \tag{3}$$

where $H(q)$ is a function of real value q, and the average is taken over all possible pairs of $(y(n+m), y(n))$. Negative and positive q values emphasize small and large absolute increments of $y(n)$, respectively. When the scaling laws described by (3) hold, the process under investigation is said to be a fractal process. Furthermore, if $H(q)$ is not a constant, the process is a multifractal; otherwise, it is a monofractal [43]–[45].

When $q = 2$, the analysis procedure described by (3) is often called fluctuation analysis (FA). It characterizes the correlation structure of the data set. In fact, when (3) for $q = 2$ holds, the autocorrelation for the increment process x decays as a power-law

$$\gamma(k) \sim k^{2H(2)-2} \quad \text{as } k \to \infty \tag{4}$$

where $H(2)$ is often called the Hurst parameter, and simply denoted as H. When $H = 1/2$, the process is called memoryless or short range dependent. The most well-known example is the Brownian motion (Bm) process. In nature and in man-made systems, often a process is characterized by an $H \neq 1/2$. Prototypical models for such processes are fractional Brownian motion (fBm) processes. When $0 \leq H < 1/2$, the process is said to have "anti-persistent" correlations [46]. For $1/2 < H \leq 1$, the process has "persistent" correlations, or long memory properties [46]. The latter is justified by noticing that

$$\sum_{k=1}^{k=\infty} \gamma(k) = \infty. \tag{5}$$

In practice, quite often power-law relations are only valid for a finite scaling region $[k_{\min}, k_{\max}]$, where both $k_{\min}$ and $k_{\max}$ are important parameters that have physical significance. Unfortunately, many researchers often try to estimate the H parameter (or other scaling exponents such as the fractal dimension) by some optimization procedure without being concerned at the scaling region at all.

By the Wiener–Khinchin theorem, one finds that if the process x is fractal, its power spectral density (PSD) has the form

$$E_x(f) \sim \frac{1}{f^{2H-1}}. \tag{6}$$

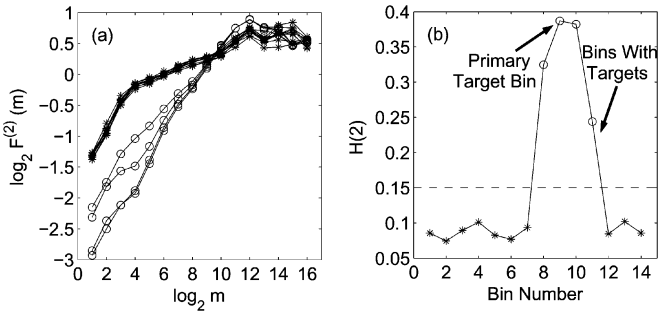

Fig. 2. (a) $\log_2 F^{(2)}(m)$ versus $\log_2 m$ for the 14 range bins. (b) The $H(2)$ values for the 14 range bins. The sea clutter data is treated as a "random walk" process. Open circles denote the range bins with target, while $*$ denote the bins without target. This rule applies to all other figures.

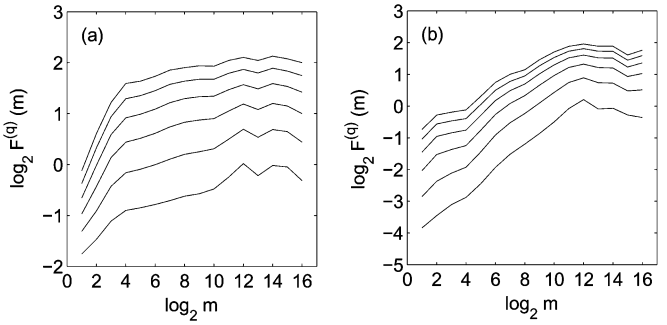

Fig. 3. Representative $\log_2 F^{(q)}(m)$ versus $\log_2 m$ curves for a number of q values for the sea clutter data (a) without and (b) with target. Curves from bottom to top correspond to $q = 1, 2, \ldots, 6$. The sea clutter data is treated as a "random walk" process.

The random walk process y has the PSD

$$E_y(f) \sim \frac{1}{f^{2H+1}}. \tag{7}$$

The processes under study are thus often called $1/f^{\alpha}$ noise. Such type of noise is very ubiquitous. For classic as well as recent examples of such processes, we refer to [47]–[49]. Mathematically, a $1/f^{\alpha}$ process is considered nonstationary when $1 < \alpha < 3$ [44], [45]. This is understandable, since Gaussian noise is stationary, while Bm (where $\alpha = 2$) is nonstationary. In fact, we shall show later, sea clutter data is weakly nonstationary in the time scale range of about 0.01 s to a few seconds.

Equation (6) or (7) offers one way of estimating the Hurst parameter. However, with such an approach, it may be difficult to determine a suitable region to define the power-law scaling.

IV. Multifractal Analysis of Sea Clutter

In practice, since one does not know *a priori* whether a measured sea clutter data should be treated as the "random walk" or the "increment" process, let us analyze them both.

A. Sea Clutter Data Treated as "Random Walk" Processes

Let us treat sea clutter data as "random walk" processes first. We can directly apply (3) by replacing $y(n)$ by the sea clutter amplitude data. Let us first focus on $q = 2$. Representative results of $\log_2 F^{(2)}(m)$ versus $\log_2 m$ for the 14 range bins of one measurement are shown in Fig. 2(a), where the curves denoted by open circles are for data with the target, while the curves denoted by asterisks are for data without the target. We observe that the curves are fairly linear in the range of $m = 2^4$ to about $m = 2^{12}$. They correspond to the time scale range of about 0.01 s to a few seconds, since the sampling frequency of the sea clutter data is 1000 Hz. Thus in this time scale range the sea clutter data can be classified as fractal. The $H(2)$ parameter of each curve can be estimated by fitting a straight line to the $\log_2 F^{(2)}(m)$ versus $\log_2 m$ curve in the range of $m = 2^4$ to $m = 2^{12}$. The estimated parameter is explicitly shown in Fig. 2(b). We notice that the $H(2)$ parameters of the curves for the data with the target are much larger than those for the data without the target. It turns out this is a generic feature for all the measurements.

Next let us examine if the data is multifractal. In Fig. 3(a) and (b), we have shown representative $\log_2 F^{(q)}(m)$ versus $\log_2 m$ curves for a number of q values for two sea clutter data, one is without the target, the other with the target. The variation of $H(q)$ versus q for the 14 range bins data of one measurement is shown in Fig. 4. We observe that the sea clutter data appear to be multifractal, especially for data with the target. The effectiveness of $H(2)$ for distinguishing data with and without the target stimulates us to examine if $H(q)$ values for other q may have similar power. This turns out to be generically true. A representative result is shown in Fig. 5. We observe that $H(q)$ values for other q are also much larger for the data with the target than for those without the target.

Let us now focus on $H(2)$ and critically examine if a robust detector for detecting targets within sea clutter can be developed based on $H(2)$. We have systematically studied 392 time series

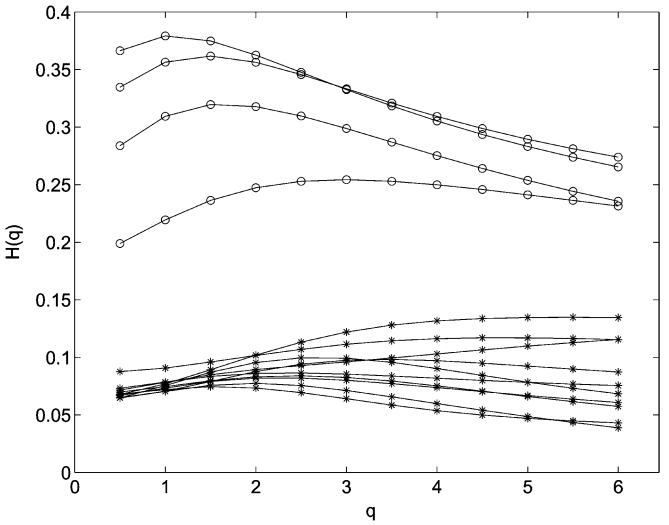

Fig. 4. Variation of $H(q)$ versus q curves for the 14 range bins. The sea clutter data is treated as a "random walk" process.

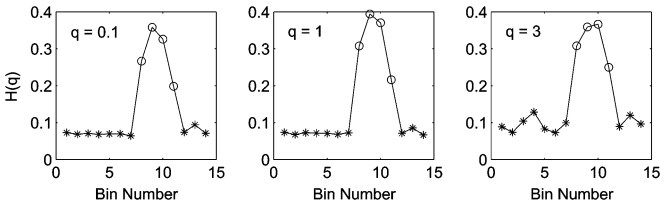

Fig. 5. $H(q)$ values for the 14 range bins, $q = 0.1$, 1, 3. The sea clutter data is treated as a "random walk" process.

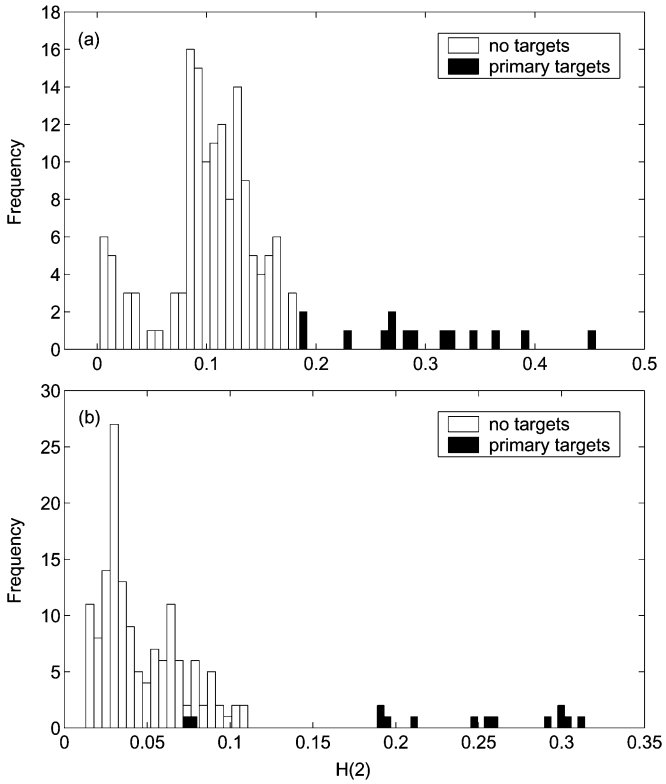

Fig. 6. Frequencies of the bins without targets and the bins with primary targets for (a) HH and (b) VV datasets. The sea clutter data are treated as "random walk" processes.

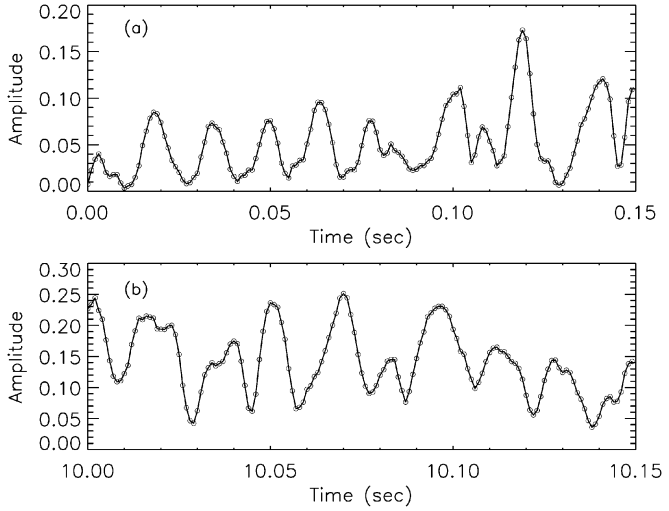

Fig. 7. Two short segments of the sea clutter amplitude data (adapted from [27], [28]).

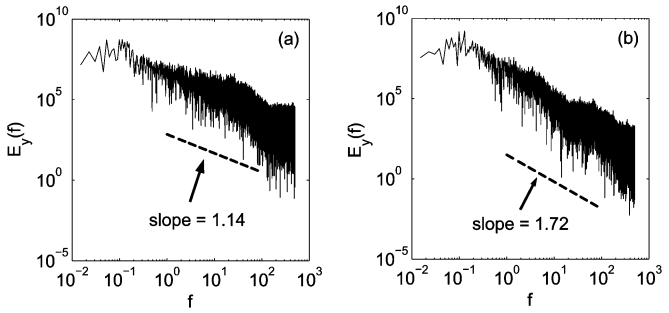

Fig. 8. (a) and (b) show the PSD corresponding to the two sea clutter data shown in Fig. 1(a) and (b), respectively.

of the sea clutter data measured under various sea and weather conditions. To better appreciate the detection performance, we have first only focused on bins with primary targets, but omitted those with secondary targets, since sometimes it is hard to determine whether a bin with secondary target really hits a target or not. After omitting the range bin data with secondary targets, the frequencies for the $H(2)$ parameter under the two hypotheses (the bins without targets and those with primary targets) for HH and VV datasets are shown in Fig. 6(a) and (b), respectively. We observe that the frequencies completely separate for the HH datasets. The accuracy for the VV datasets is also very good, except for two measurements. Interestingly, those measurements correspond to the two HH measurements with the two smallest $H(2)$ values.

What is the physical significance of the two time scales, one about 0.01 s and the other around a few seconds, identified in our fractal scaling analysis? We observe that for time scale up to 0.01 s, the amplitude waveform of sea clutter is fairly smooth, as can be evidently seen from Fig. 7. The time scale of a few seconds may correspond to how fast the wave pattern on the sea surface changes. These time scales may slightly change with sea and wind conditions. Interestingly, these two time scales have been explicitly accounted for by the compound-Gaussian model [50], where the time scale of a few seconds is considered as the decorrelation time of the texture.

Our analysis indicates that the sea clutter data is a type of $1/f^{\alpha}$ noise with $\alpha = 2H + 1$ corresponding to the time scale range of around 0.01 s to a few seconds. It is interesting to estimate the PSD of sea clutter to check whether it indeed decays as a power-law in the frequency range corresponding to the time scale range identified. If yes, one should check whether the Hurst parameter estimated by the spectral analysis is consistent with that by fractal scaling analysis.

We have systematically estimated the PSD from all the sea clutter data. Two representative PSD curves are shown in Fig. 8 in log-log coordinates. The dashed straight lines in Fig. 8 are in the frequency range of 1 to 100 Hz, which corresponds to the time scale range identified earlier. Those two straight lines are obtained by the least-squares fit to the PSD curves in that frequency range. The slopes are 1.14 and 1.72, which are equivalent to $H = 0.07$ and 0.36. The Hurst parameters for the same datasets estimated by fractal scaling analysis are 0.07 and 0.37. They are almost identical.

Recalling that a $1/f^{\alpha}$ process is nonstationary when $1 < \alpha < 3$ [44], [45], we thus conclude that sea clutter data is weakly nonstationary in the time scale range of about 0.01 s to a few seconds. We will discuss its implications in Section VI.

B. Sea Clutter Data Treated as "Increment" Processes

Let us now consider the measured sea clutter data as "increment" processes. Before we can apply (3), we have to first remove the mean value, and then form the partial summation, as defined by (1) and (2). A representative result of $\log_2 F^{(2)}(m)$ versus $\log_2 m$ is shown in Fig. 9(a) and the $H(2)$ values shown in Fig. 9(b). We observe that the scaling relations become better.

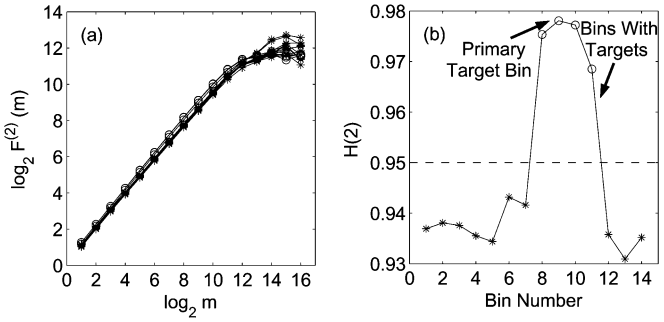

Fig. 9. (a) $\log_2 F^{(2)}(m)$ versus $\log_2 m$ for the 14 range bins. (b) $H(2)$ values for the 14 range bins. The sea clutter data is considered as an "increment" process.

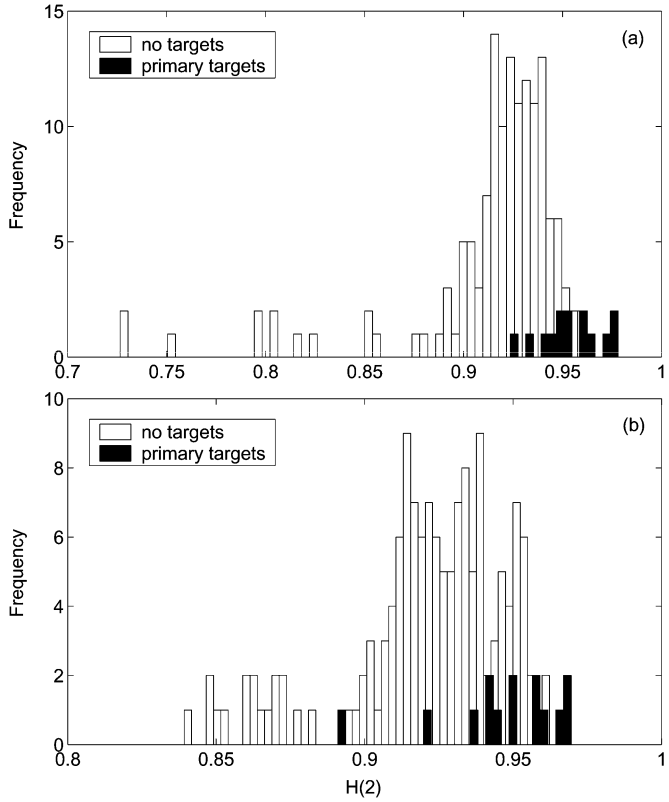

Fig. 10. Frequencies of the bins without targets and the bins with primary targets for (a) HH and (b) VV datasets. The sea clutter data are considered as "increment" processes.

While the variation of $H(2)$ versus the range-bin number still indicates which bins hit the target, overall, the $H(2)$ values are very close to 1. Because of this, fractal scaling analysis becomes ineffective for the purpose of distinguishing sea clutter data with and without targets. This can be readily seen from Fig. 10, where the PDF of the $H(2)$ parameters for the data without targets significantly overlaps with that for the data with targets.

Let us explain why FA may fail for detecting targets within sea clutter. This lies in the observation that the largest Hurst parameter given by FA is 1. To explain the idea, let us assume $y(n) \sim n^{\beta}$, $\beta > 1$. Then $\langle |y(n+m) - y(n)|^2 \rangle = \langle [(n+m)^{\beta} - n^{\beta}]^2 \rangle$ is dominated by terms with large n. When this is the case, $(n+m)^{\beta} = [n(1+m/n)]^{\beta} \approx n^{\beta}[1+\beta m/n]$. One then sees that $\langle |y(n+m) - y(n)|^2 \rangle \sim m^2$, i.e., $H(2) = 1$. We call this the saturation phenomenon associated with FA. An important implication of this discussion is that whenever one observes a Hurst parameter very close to 1, one has to be alerted that it may be advantageous to re-do the analysis by treating the original time series as a "random walk" process instead of an "increment" process.

V. Distributional Analysis of Sea Clutter

A number of distributions have been proposed to model sea clutter data, including Weibull [1], log-normal [2]–[4], K [5]–[8], [12], and compound-Gaussian [9], [10] distributions. Since we are not aware of any published systematic study on the effectiveness of those distributions for detecting targets within sea clutter, to appreciate this issue better, we have carried out such an analysis. Our analysis may also serve the purpose of comparing the performance of target detection based on distributional analysis and fractal scaling analysis. There exist many different ways for estimating parameters of these PDFs. We are aware that the parameters we have chosen may not be the best for certain sea clutter data.

Let us briefly describe the four distributions that we have carefully examined.

(i) Weibull distribution:

One preferred PDF form with two parameters can be expressed as

$$f(x) = abx^{b-1}e^{-ax^b}, \quad x \geq 0, \ a > 0, \ b > 0. \tag{8}$$

One robust way to estimate the parameters is to fit each sample dataset with the following straight line relationship (in log-log coordinates) [51]:

$$\ln(-\ln(1 - F(x))) = b \ln x + \ln a \tag{9}$$

where $F(x)$ is the cumulative distribution function (CDF). As we can see, b is the slope of the line and $\ln a$ is its intercept at the y-axis.

(ii) log-normal distribution:

Its PDF is given by

$$f(x) = \frac{1}{(2\pi)^{1/2}\sigma x} e^{(-(\ln x - \mu)^2)/2\sigma^2}, \quad x > 0 \tag{10}$$

where μ, σ are, respectively, the mean and the standard deviation of the logarithm of random variable x. A straight-line relationship can also be derived to check the fitness of log-normal distribution [51]

$$erf^{-1}(2F(x) - 1) = \frac{(\ln x - \mu)}{\sqrt{2}\sigma} \tag{11}$$

where erf is the error function.

(iii) K distribution:

Its PDF is given by [52]

$$f(x) = \frac{\sqrt{2\nu}}{\sqrt{\mu}\Gamma(\nu)2^{\nu-1}} \left(\sqrt{\frac{2\nu}{\mu}}x\right)^{\nu} K_{\nu-1}\left(\sqrt{\frac{2\nu}{\mu}}x\right), \quad x \geq 0. \tag{12}$$

The moments for K distribution are [52]

$$E\{x^n\} = \frac{(2\mu)^{n/2}\Gamma\left(\nu+\frac{n}{2}\right)\Gamma\left(\frac{n}{2}+1\right)}{\nu^{n/2}\Gamma(\nu)}, \quad n=1,2,\ldots \tag{13}$$

The characteristic parameters of the theoretical K distribution have been estimated by the method of moments from the following relations [50]:

$$\frac{E\{x^2\}}{E^2\{x\}} = \frac{4\nu\Gamma^2(\nu)}{\pi\Gamma^2(\nu+0.5)}, \quad E\{x^2\}=2\mu. \tag{14}$$

(iv) Compound-Gaussian distribution:

This distribution decomposes a random variable x into the product of two other random variables $x = \sqrt{\tau}z$. For sea clutter data, z is a locally Rayleigh component, referred to as speckle, and τ is a Gamma component, which modulates the power level relative to the underlying sea swell, referred to as texture. The Gamma PDF is given by

$$p_\tau(\tau) = \frac{1}{\Gamma(\nu)}\left(\frac{\nu}{\mu}\right)^\nu \tau^{\nu-1}\exp\left(-\frac{\nu}{\mu}\tau\right), \quad \tau \geq 0. \tag{15}$$

The two components z and τx are suggested to have two different decorrelation times [50]. The Rayleigh component of sea clutter typically decorrelates in about 0.01 s, whereas the texture can have decorrelation times on the order of several seconds. These two time scales are quite consistent with the time scales identified by fractal scaling analysis. We follow the method given in [50] to do the compound-Gaussian distribution analysis.

Given a theoretical distribution with its parameters properly estimated for a particular dataset, a goodness-of-fit test can be performed to determine whether the data plausibly can have arisen from that distribution. We employ the Kolmogorov–Smirnov (KS) one-sample test [53], which is based on the maximum deviation of the empirical CDF from the theoretical one

$$D_e = \max_{1\leq i\leq N} |F(x_i) - F_t(x_i)| \tag{16}$$

where $F(x_i)$ is the empirical CDF, its value equals to i/N, where i is the number of data points not larger than x_i and N is the total number of data points. The corresponding theoretical CDF, $F_t(x_i)$, is calculated for the candidate distribution with its parameters estimated for that particular dataset. D_e can be compared against the critical value D_{crit} associated with the chosen level of significance ($p < 0.05$) and the sample size (N). If D_e is greater than D_{crit}, then the null hypothesis will be rejected and the data cannot plausibly be thought of as arising from the specified distribution.

We have carefully examined whether the parameters estimated from the four distributions and the corresponding D_e values can be used for distinguishing sea clutter data with and without targets. It is found that within some measurements, the parameters of some distributions can indeed be used for this purpose. However for any of the four distributions, there exists at least one measurement that this approach does not work. One example is shown in Fig. 11 for the K distribution. Based on Fig. 11(a) and (b), we conclude that it is impossible to tell which range bin hits the target from either the ν parameters or the D_e values. The behavior of the other three distributions is quite similar to that of K distribution. Since distributional analysis is not even able to detect targets within sea clutter in a single measurement, we conclude that fractal scaling analysis is much more effective for detecting targets within sea clutter.

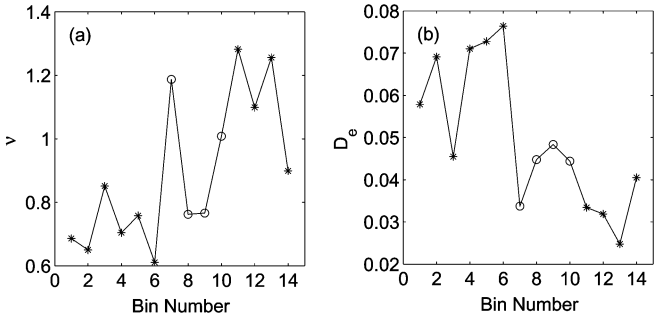

Fig. 11. (a) ν parameters and (b) D_e values obtained from the K distribution for the 14 range bins.

VI. Conclusion and Discussions

We have introduced the structure function based multifractal technique for detecting small low observable targets within sea clutter. We have systematically studied 392 amplitude time series of the sea clutter data measured under various sea and weather conditions, and found that sea clutter data exhibit multifractal behaviors in the time scale range of about 0.01 s to a few seconds. More importantly, we have found that the $H(q)$ spectrum can accurately determine whether a range bin hits a target or not. Intuitively, one would think it more difficult to detect smaller targets than larger ones. The smallness of the target detected here (about 1 m) thus highly suggests that our method will work equally well or even better for detecting targets of much larger size, such as vessels. We also note that our data was measured more than 10 years ago. We have found that the quality of the data is not very good, for example, some datasets were severely clipped. With the availability of new techniques of measuring high quality data, we expect our method may become more effective. Most importantly, since the method does not require any training, and is simple and computationally fast, it may be readily developed into an automated target detector within sea clutter for real-time operation.

We emphasize that the fractal scaling behavior identified from sea clutter data is only valid within the time scale range of about 0.01 s and a few seconds. We have shown that below 0.01 s, the amplitude waveform of sea clutter data is fairly smooth. We have also conjectured that the time scale of a few seconds may correspond to how fast the wave pattern on the sea surface may change. It is possible that these time scales may slightly change with sea and wind conditions.

An important finding of our study is that sea clutter data is weakly nonstationary in the time scale range of 0.01 s to a few seconds. This may have explained why distributional analysis has only offered limited understanding so far and is not very effective for target detection within sea clutter. This may imply that distributional analysis better be performed based on the

analysis of the increment process of sea clutter data obtained by differencing. Pleasingly, we have obtained some promising results by fitting increment processes to the Tsallis distribution, which is closely related to α-stable-type distributions (see [54], [55]). This is still work in progress though, and will be reported in the near future.

The existence of the time scales of 0.01 s and a few seconds does not mean that other time scales may not exist. In fact, we believe that the multifractal analysis procedure discussed here may reveal additional time scales, when it is applied to much longer time series data (such as 10 mins to half an hour long). This remains to be seen in the future.

Finally, we mention that the analysis can be extended to spatial domain, such as images from remote sensing. In those situations, m becomes a spatial scale.

REFERENCES

[1] F. A. Fay, J. Clarke, and R. S. Peters, "Weibull distribution applied to sea-clutter," in *Proc. Inst. Elect. Eng. Conf. Radar'77*, London, U.K., 1977, pp. 101–103.

[2] F. E. Nathanson, *Radar Design Principles*: McGraw Hill, 1969, pp. 254–256.

[3] G. V. Trunk and S. F. George, "Detection of targets in non-Gaussian sea clutter," *IEEE Trans. Aerosp. Electron. Syst.*, vol. 6, pp. 620–628, 1970.

[4] H. C. Chan, "Radar sea-clutter at low grazing angles," *Proc. Inst. Elect. Eng.*, vol. F137, pp. 102–112, 1990.

[5] E. Jakeman and P. N. Pusey, "A model for non Rayleigh sea echo," *IEEE Trans. Antennas Propag.*, vol. 24, pp. 806–814, 1976.

[6] K. D. Ward, C. J. Baker, and S. Watts, "Maritime surveillance radar part 1: Radar scattering from the ocean surface," *Proc. Inst. Elect. Eng.*, vol. F137, pp. 51–62, 1990.

[7] T. Nohara and S. Haykin, "Canadian east coast radar trials and the K-distribution," *Proc. Inst. Elect. Eng.*, vol. F138, pp. 80–88, 1991.

[8] F. Gini, M. Montanari, and L. Verrazzani, "Maximum likelihood, ESPRIT, and periodogram frequency estimation of radar signals in K-distributed clutter," *Signal Processing*, vol. 80, pp. 1115–1126, 2000.

[9] F. Gini, "Performance analysis of two structured covariance matrix estimators in compound-Gaussian clutter," *Signal Processing*, vol. 80, pp. 365–371, 2000.

[10] F. Gini, A. Farina, and M. Montanari, "Vector subspace detection in compound-Gaussian clutter, part II: Performance analysis," *IEEE Trans. Aerosp. Electron. Syst.*, vol. 38, pp. 1312–1323, 2002.

[11] F. L. Posner, "Spiky sea clutter at high range resolutions and very low grazing angles," *IEEE Trans. Aerosp. Electron. Syst.*, vol. 38, pp. 58–73, 2002.

[12] S. Sayama and M. Sekine, "Log-normal, log-Weibull and K-distributed sea clutter," *IEICE Trans. Commun.*, vol. E85-B, pp. 1375–1381, 2002.

[13] A. I. Morrison and M. A. Srokosz, "Estimating the fractal dimension of the sea-surface—A 1st attempt," *Annales Geophysicae-Atmospheres Hydrospheres and Space Sci.*, vol. 11, pp. 648–658, 1993.

[14] M. Martorella, F. Berizzi, and E. D. Mese, "On the fractal dimension of sea surface backscattered signal at low grazing angle IEEE," *IEEE Trans. Antennas Propag.*, vol. 52, pp. 1193–1204, 2004.

[15] F. Berizzi, E. Dalle-Mese, and M. Martorella, "A sea surface fractal model for ocean remote sensing," *Int. J. Remote Sensing*, vol. 25, pp. 1265–1270, 2004.

[16] S. Savaidis, P. Frangos, D. L. Jaggard, and K. Hizanidis, "Scattering from fractally corrugated surfaces: An exact approach," *Opt. Lett.*, vol. 20, pp. 2357–2359, 1995.

[17] X. Sun and D. L. Jaggard, "Wave scattering from nonrandom fractal surfaces," *Opt. Commun.*, vol. 78, pp. 20–24, 1990.

[18] F. Berizzi and E. Dalle-Mese, "Scattering from a 2-D sea fractal surface: Fractal analysis of the scattered signal," *IEEE Trans. Antennas Propag.*, vol. 50, pp. 912–925, 2002.

[19] G. Franceschetti, A. Iodice, M. Migliaccio, and D. Riccio, "Scattering from natural rough surfaces modeled by fractional brownian motion two-dimensional processes," *IEEE Trans. Antennas Propag.*, vol. 47, pp. 1405–1415, 1999.

[20] S. Haykin and S. Puthusserypady, "Chaotic dynamics of sea clutter," *Chaos*, vol. 7, pp. 777–802, 1997.

[21] S. Haykin, *Chaotic Dynamics of Sea Clutter*. New York: Wiley, 1999.

[22] S. Haykin, R. Bakker, and B. W. Currie, "Uncovering nonlinear dynamics-the case study of sea clutter," *Proc. IEEE*, vol. 90, pp. 860–881, 2002.

[23] [Online]. Available: http://www.aspc.qinetiq.com/Events/July99/abstracts.html#Cowper

[24] M. R. Cowper and B. Mulgrew, "Nonlinear processing of high resolution radar sea clutter," in *Proc. IJCNN*, vol. 4, 1999, pp. 2633–2633.

[25] M. Davies, "Looking for nonlinearities in sea clutter," in *Proc. Inst. Elect. Eng. Radar and Sonar Signal Processing*, Peebles, Scotland, Jul. 1998.

[26] J. L. Noga, "Bayesian state-space modeling of spatio-temporal non-Gaussian radar returns," Ph.D. dissertation, Cambridge Univ., 1998.

[27] J. B. Gao and K. Yao, "Multifractal features of sea clutter," in *IEEE Radar Conf.*, Long Beach, CA, Apr. 2002.

[28] J. B. Gao, S. K. Hwang, H. F. Chen, Z. Kang, K. Yao, and J. M. Liu, "Can sea clutter and indoor radio propagation be modeled as strange attractors?," in *Proc. 7th Experimental Chaos Conf.*, San Diego, CA, Aug. 2002, pp. 25–29.

[29] M. McDonald and A. Damini, "Limitations of nonlinear chaotic dynamics in predicting sea clutter returns," *Proc. Inst. Elect. Eng.-Radar. Son. Nav.*, vol. 151, pp. 105–113, 2004.

[30] T. Thayaparan and S. Kennedy, "Detection of a manoeuvring air target in sea-clutter using joint time-frequency analysis techniques," *Proc. Inst. Elect. Eng.-Radar, Sonar and Navigation*, vol. 151, pp. 19–30, 2004.

[31] G. Davidson and H. D. Griffiths, "Wavelet detection scheme for small targets in sea clutter," *Electron. Lett.*, vol. 38, pp. 1128–1130, 2002.

[32] T. Bhattacharya and S. Haykin, "Neural network-based adaptive radar detection scheme for small ice targets in sea clutter," *Electron. Lett.*, vol. 28, pp. 1528–1529, 1992.

[33] ——, "Neural network-based radar detection for an ocean environment," *IEEE Trans. Aerosp. Electron. Syst.*, vol. 33, pp. 408–420, 1997.

[34] H. Leung, N. Dubash, and N. Xie, "Detection of small objects in clutter using a GA-RBF neural network," *IEEE Trans. Aerosp. Electron. Syst.*, vol. 38, pp. 98–118, 2002.

[35] N. Xie, H. Leung, and H. Chan, "A multiple-model prediction approach for sea clutter modeling," *IEEE Trans. Geosci. Remote.*, vol. 41, pp. 1491–1502, 2003.

[36] C. P. Lin, M. Sano, S. Sayama, and M. Sekine, "Detection of radar targets embedded in sea ice and sea clutter using fractals, wavelets, and neural networks," *IEICE Trans. Commun.*, vol. E83B, pp. 1916–1929, 2000.

[37] C. P. Lin, M. Sano, S. Obi, S. Sayama, and M. Sekine, "Detection of oil leakage in SAR images using wavelet feature extractors and unsupervised neural classifiers," *IEICE Trans. Commun.*, vol. E83B, pp. 1955–1962, 2000.

[38] T. Lo, H. Leung, J. Litva, and S. Haykin, "Fractal characterization of sea-scattered signals and detection of sea-surface targets," *Proc. Inst. Elect. Eng.*, vol. F140, pp. 243–250, 1993.

[39] C.-P. Lin, M. Sano, and M. Sekine, "Detection of radar targets by means of fractal error," *IEICE Trans. Commun.*, vol. E80-B, pp. 1741–1748, 1997.

[40] B. E. Cooper, D. L. Chenoweth, and J. E. Selvage, "Fractal error for detecting man-made features in aerial images," *Electron. Lett.*, vol. 30, pp. 554–555, 1994.

[41] D. Gan and Z. Shouhong, "Detection of sea-surface radar targets based on multifractal analysis," *Electron. Lett.*, vol. 36, pp. 1144–1145, 2000.

[42] D. C. Kim, S. Sayama, and M. Sekine, "Detection of target embedded in sea clutter by means of millimeter wave radar," *Int. J. Infrared Millimeter Waves*, vol. 24, pp. 1499–1508, 2003.

[43] G. Parisi and U. Frisch, *Turbulence and Predictability in Geophysical Fluid Dynamics and Climate Dynamics*, M. Ghil, R. Benzi, and G. Parisi, Eds. Amsterdam, The Netherlands: North-Holland, 1985, pp. 84–84.

[44] A. Davis, A. Marshak, W. Wiscombe, and R. Cahalan, "Multifractal characterizations of nonstationarity and intermittency in geophysical fields, observed, retrieved or simulated," *J. Geophys. Res.*, vol. 99, pp. 8055–8072, 1994.

[45] ——, *Current Trends in Nonstationary Analysis*, G. Trevilo, J. Hardin, B. Douglas, and E. Andreas, Eds, Singapore: World Scientific, 1996, pp. 97–158.

[46] B. B. Mandelbrot, *The Fractal Geometry of Nature*. San Francisco, CA: Freeman, 1982.

[47] W. H. Press, "Flicker noises in astronomy and elsewhere," *Comments on Astrophysics*, vol. 7, pp. 103–119, 1978.

[48] P. Bak, *How Nature Works: The Science of Self-Organized Criticality*. Katlenburg-Lindau, Germany: Copernicus, 1996.
[49] J. B. Gao, Y. Cao, and J.-M. Lee, "Principal component analysis of $1/f^{\alpha}$ noise," *Phys. Lett. A*, vol. 314, pp. 392–400, 2003.
[50] A. Farina, F. Gini, M. V. Greco, and L. Verrazzani, "High resolution sea clutter data: Statistical analysis of recorded live data," *Proc. Inst. Elect. Eng.-Radar, Sonar Navig.*, vol. 144, pp. 121–130, 1997.
[51] Y. H. Zhou, J. B. Gao, K. D. White, I. Merk, and K. Yao, "Perceptual dominance time distributions in multistable visual perception," *Biol. Cybern*, vol. 90, pp. 256–263, 2004.
[52] A. Stuart and J. K. Ord, *Kendall's Advanced Theory of Statistics*: Griffin, 1987, vol. 1.
[53] S. Siegel, *Non-Parametric Statistics for the Behavioral Sciences*. New York: McGraw-Hill, 1956.
[54] C. Tsallis, S. V. F. Levy, A. M. C. Souza, and R. Maynard, "Statistical-Mechanical foundation of the ubiquity of lévy distributions in nature," *Phys. Rev. Lett.*, vol. 75, pp. 3589–3593, 1995.
[55] C. Beck, G. S. Lewis, and H. L. Swinney, "Measuring nonextensitivity parameters in a turbulent couette-Taylor flow," *Phys. Rev. E*, vol. 63, pp. 035 303(R)–035 303(R), 2001.

Jing Hu received the B.Sc. and M.Eng. degrees in electrical engineering from Huazhong University of Science and Technology, Wuhan, China, in 2000 and 2002, respectively. She is currently pursuing the Ph.D. degree in electrical and computer engineering from the University of Florida, Gainesville.

Her research interests include signal processing, chaos and fractal time series analysis, radar systems, biological data analysis, and bioinformatics.

Wen-Ww Tung is an Assistant Professor in the Department of Earth and Atmospheric Sciences at Purdue University, West Lafayette, IN. Her research is focused on diagnosing and modeling the Earth's regional climate systems with an emphasis on the effects of clouds in the systems, with approaches which are both analytical/physical and systemic. On the one hand, physical models are used with multiscale nesting techniques in order to study cloud systems in a synoptic setting, such as the convective systems over the Bay of Bengal, which are energetically important to the South Asian monsoon. On the other hand, statistical methods, nonlinear dynamics theory, fractal geometry, and wavelet based tools are employed to analyze observations as well as model results in order to systemically characterize the exquisitely complicated cloud-coupled climate systems and challenge our current understandings of these systems.

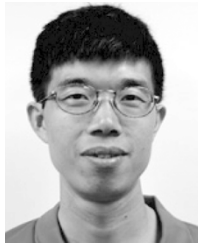

Jianbo Gao (M'00) received the Ph.D. degree from the University of California, Los Angeles, in 2000.

He is an Assistant Professor at the University of Florida, Gainesville.

He has been working on a number of different fields including nano- and fault-tolerant computing, nonlinear time series analysis, traffic modeling in communications networks, nonlinear dynamics of the Internet, characterization of non-Gaussian noise in radio communications channels, and bioinformatics. Some of the tools he developed have been applied to study a wide range of real world signal processing problems arising from as diverse fields as physics, geophysics, biology, economics, and engineering.